Proceedings of the 9th World Congress on Momentum, Heat and Mass Transfer (MHMT'24)
London, United Kingdom – April 11-13, 2024
Paper No. ENFHT 219
DOI: 10.11159/enfht24.219

Shape and Layout Optimization of Bare-Tube Heat Exchangers Using the Adjoint Method and CAD-based Parametrization

Praharsh Pai Raikar[1,2], Octavian Bociar[2], Carlo De Servi[1,2], Nitish Anand[1]
[1]VITO
Boeretang 200, Mol, 2400, Belgium
praharsh.pairaikar@vito.be
nitish.anand@vito.be
[2]Delft University of Technology
Kluyverweg 1, Delft, 2629HS, The Netherlands
g.o.bociar@student.tudelft.nl
c.m.deservi@tudelft.nl

Abstract –This study presents a Computational Fluid Dynamics (CFD)-based optimization framework to enhance the performance of bare-tube heat exchangers. The framework comprises a CFD solver, an adjoint solver, and a CAD-based parametrization tool. This framework simultaneously optimizes the tube shape and layout to obtain an optimum heat exchanger configuration with a higher heat transfer rate and lower pressure drop. Firstly, a parametric study of the longitudinal pitch is performed that shows that increasing the longitudinal pitch results in an increase in pressure drop and heat transfer rate. Furthermore, the proposed framework was applied to optimize an in-line elliptical tube configuration. The optimum geometry showed a performance improvement of 29% as compared to the baseline geometry while satisfying the constraint on the heat transfer rate.

Keywords**:** Design and Simulation, CFD, Turbulent Flow and Heat Transfer, Drag Reduction, Shape Optimization.

1. Introduction

Heat exchangers are crucial devices of energy conversion systems as the overall conversion efficiency is directly linked to the effectiveness of the heat exchangers used in the thermodynamic process. Ideally, heat exchangers should feature a high heat transfer rate per unit area, low pressure drop, and minimal weight and volume [1]. Recently, heat exchangers made up of bare tubes of small diameter have emerged as suitable heat exchanger technology for mobile applications [2], for example, road vehicles and aircraft. This is primarily due to the relatively high heat transfer coefficient per unit of volume, consequently resulting in compact heat exchangers [3][4].

The design of the bare-tube heat exchangers involves selecting the shape and the layout of the tubes. Conventional tubes may feature round [5], oval [6], elliptical [7], or tear-drop [8] shapes. The selection of the tube shape is usually driven by the chosen manufacturing method, the Reynolds number at which the tube bundle operates, and the thermal-hydraulic performance of the heat exchanger targeted in the design. Studies have established that elliptical and drop-shaped bare-tube heat exchangers have a better thermal-hydraulic performance, whereas round and oval tubes are more popular because of their simpler manufacturing method. The layout of the bare-tube heat exchangers is defined by the longitudinal and transverse pitches. The optimal value of these parameters is usually obtained by conducting parametric studies, where the longitudinal and transverse pitches are varied for a range of Reynolds numbers to study the trend between heat exchanger size and pressure drops in the cold and hot streams. For example, in Ref. [9][10], a parametric study was performed to achieve a high Nusselt number and low friction factor for rounded bare-tube heat exchangers. Overall, these parametric studies have been instrumental in providing insights into the performance of bare tube heat exchangers under varying conditions. However, they involve trial-and-error and do not necessarily lead to optimal designs.

Another way to obtain the optimal shape and layout configuration for bare-tube heat exchangers is by using optimization. For example, Lim et al. [2] used the multi-objective genetic algorithm (MOGA) to obtain a Pareto front of round tube designs, whose objective functions were the air-side pressure drop and heat transfer rate. The heat exchanger model in Ref. [2], was

based on the analytical ϵ-NTU method and empirical correlations for heat transfer coefficient and friction factor. Conversely, Kasagi et al. [11] used a neural network trained on the results of a CFD model to estimate the heat transfer rate and pressure drop across bundles of round tubes for a wide range of tube longitudinal pitch, transverse pitch and Reynolds numbers. The results show that optimal values of dimensionless transverse and longitudinal tube pitch were 2.28 and 1.31 respectively. While the previous optimization studies dealt with round tubes only, Bacellar et al. [4] presented non-round tubes whose shape and layout were optimized by using MOGA. The performance of the designs was evaluated with a CFD-based metamodel developed using the Kriging method. However, developing a metamodel is computationally expensive, especially as the number of design variables is increased to explore a larger design freedom. An alternative method enabling shape optimization in a drastically shorter computational time than MOGA is adjoint-based CFD optimization.

In this context, the aim of the research presented in this manuscript is to apply an adjoint-based CFD optimization framework to optimize the shape and layout of bare-tube heat exchangers simultaneously. Such an optimization framework was previously developed for turbomachinery problems [12][13] and was recently extended to design tube bundles [14]. This work extends this framework further by including the tube longitudinal pitch among the optimization variables. The framework is based on the open-source CFD suite SU2 [15], whose key feature is the integration of RANS solvers with an adjoint solver to determine in a computationally efficient way the gradients associated with design variables, consequently, enabling the use of gradient-based optimization methods. The other element of the optimization framework is a CAD-based parametrization [13] to represent the heat exchanger geometry, and to modify the shape and layout of the tubes during the optimization process.

To demonstrate the potential of the developed framework, an in-line elliptical bare-tube heat exchanger is selected as the test case. The numerical model is validated against data in the literature about heat transfer rate and pressure drop across in-line circular tubes. A parametric study is carried out to study the influence of the longitudinal pitch on the performance of in-line elliptical bare-tube heat exchanger. Finally, the shape and pitch of the baseline design is optimized based on 2-D flow simulations. The objective of the optimization was to reduce the pressure drop while constraining the heat transfer rate and internal area of the tubes.

2. Methodology

The proposed optimization framework utilizes the CFD and adjoint solver of the SU2 suite [15] and the CAD parametrization tool described in Ref. [13]. The framework can be represented with the help of the extended design structure matrix (XDSM) diagram illustrated in Figure 1. The XDSM diagram showcases the key components of the design chain, namely, the surface generator, mesh deformer, flow solver, adjoint solver and the optimizer. The input provided to the optimization loop is the initial design vector (α^0) and the corresponding mesh $\left(X_{vol}^0\right)$. At each optimization step, the CFD and adjoint solvers are used to determine the value of the objective function (J), flow constraint $\left(c_f\right)$, geometric constraints $\left(c_g\right)$ and their associated sensitivities. The sensitivity of the objective function with respect to the design variable can be obtained by the following matrix multiplication

$$\frac{\partial J}{\partial \boldsymbol{\alpha}} = \frac{\partial J}{\partial \boldsymbol{X_{vol}}} \cdot \frac{\partial \boldsymbol{X_{vol}}}{\partial \boldsymbol{X_{surf}}} \cdot \frac{\partial \boldsymbol{X_{surf}}}{\partial \boldsymbol{\alpha}}. \tag{1}$$

The evaluation of cost functions and gradients with respect to the design variables are performed as per Ref. [14].

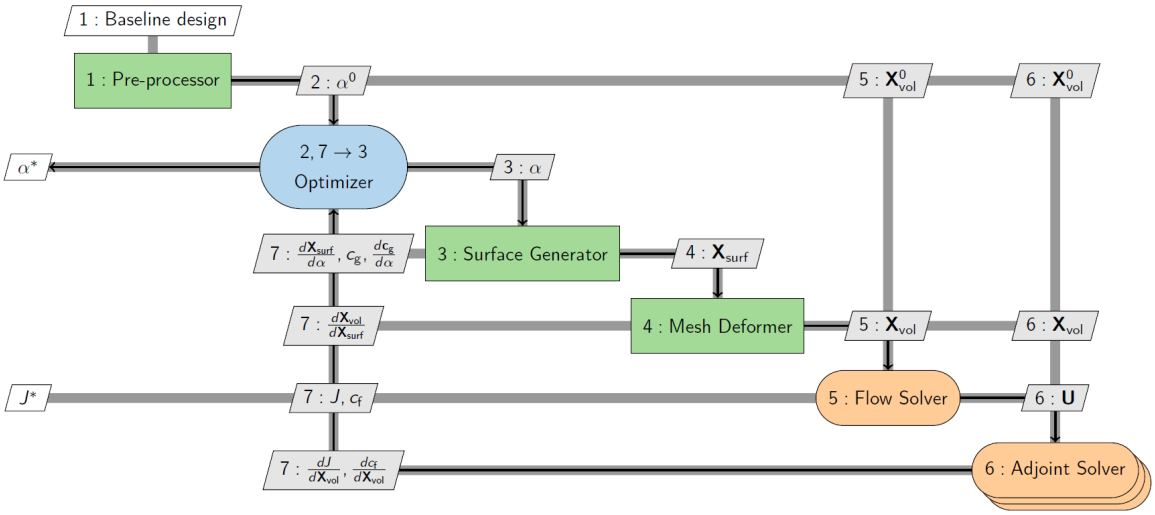

Figure 1: XDSM diagram representing the adopted optimization framework, from Ref. [14].

3. Case Study

In order to assess the capability of the optimization framework, a test case inspired by the work presented in Ref. [4] was chosen. The heat exchanger geometry consists of four elliptical tubes in an in-line arrangement, see Figure 2. The elliptical tubes have a major axis of 3 mm and a minor axis of 0.9 mm.

The computational domain and boundary conditions corresponding to this baseline geometry are shown in Figure 2. The flow domain was discretized using quadrilateral elements close to the wall and triangular elements in the rest of the domain. The mesh selected after performing a grid-independence study, consists of approximately 86,200 elements which corresponds to a 0.4% uncertainty in pressure drop due to the discretization error. Figure 3 depicts the mesh used in the simulations for analysis and design.

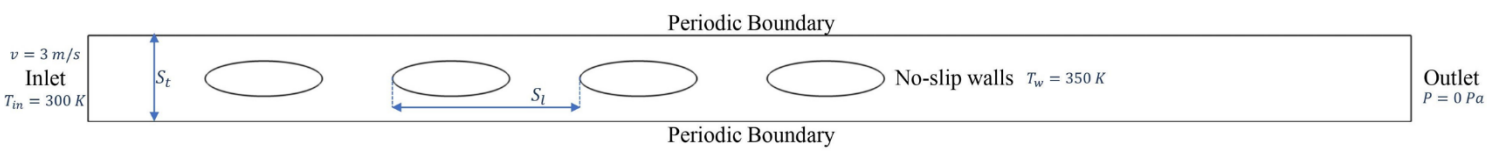

Figure 2: Computational domain and boundary conditions for the in-line elliptical tube test cases.

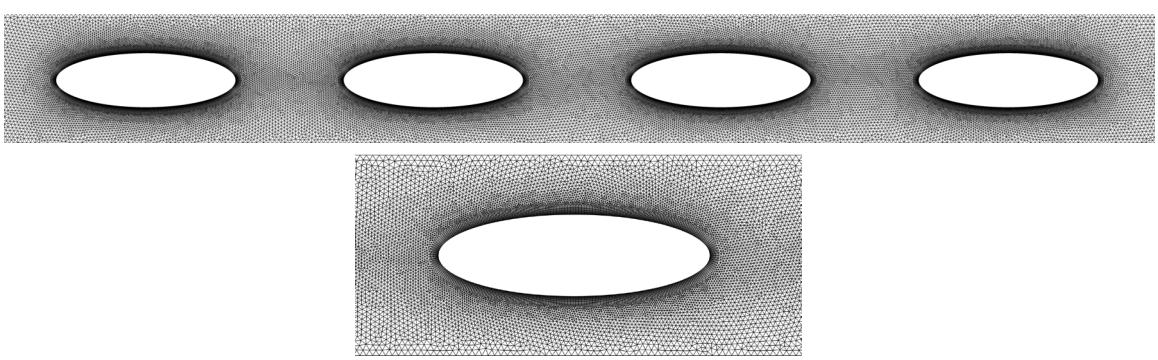

Figure 3: Discretized domain around the tubes (top) with an enlarged view of the grid (bottom).

4. Optimization Setup

The objective of the optimization is to minimize the airside pressure drop (ΔP_{air}) across the bare tubes by changing the design variables (α); while constraining the heat transfer rate ($\dot{Q}$) and the area enclosed (a) within each tube of the geometry. The optimization problem can be expressed as

$$\min_{\alpha} \quad \Delta P_{air}(\alpha), \tag{2}$$

$$s.t. \quad \dot{Q} \geq 0.97\dot{Q}_o, \tag{3}$$

$$a \geq a_o, \tag{4}$$

where $\dot{Q}_o$ is the heat transfer rate of the baseline design and a_o is the area enclosed within each tube of the baseline geometry. The framework used the SLSQP [16] optimization algorithm available within the python SciPy package [17].

5. Results

The results are presented in three separate sections. First, a validation study of the numerical setup used for the simulation is documented. Next, a parametric analysis is reported to study the effect of longitudinal pitch on the performance of the considered tube bundle. Finally, the results of the optimization are described.

5.1. Validation study

To validate the numerical model used to simulate the flow and heat transfer, a test case with in-line cylindrical tubes from Ref. [11] was selected. The geometry of this test case consists of 21 streamwise circular tubes of 0.5mm diameter in an in-line arrangement with transverse and longitudinal pitch ratios of 2.28 and 1.31 respectively. The flow conditions of the experiment considered for the validation correspond to a Reynolds number of 100 [11].

The air-side pressure drop and heat transfer coefficient estimated by the CFD model are equal to 37.1 Pa and 128.6 W/m^{2}K, respectively, versus 41.6 Pa and 136.2 W/m^{2}K of the experiment. Hence, the simulation underpredicts the heat transfer coefficient by 5.5%, and the pressure drop by 11%. The CFD model is, then, deemed sufficiently accurate for the purpose of this study.

5.2. Influence of Reynolds number and longitudinal pitch

To study the influence of longitudinal pitch, its ratio (P_l), i.e. the ratio between the longitudinal pitch and the major axis of the ellipse, was varied from 1.25 to 4. The key performance parameters considered for this parametric study are the Nusselt number (Nu) and the Euler number (Eu), representing the non-dimensional heat transfer coefficient and the pressure drop (ΔP), respectively. The definition of these quantities is as follows:

$$Re = \frac{v\rho L}{\mu}, \tag{5}$$

$$Eu = \frac{\Delta P}{\frac{1}{2}v^2\rho}, \tag{6}$$

$$Nu = \frac{hL}{k}, \tag{7}$$

$$h = \frac{\dot{m}c_p}{A_w} ln\left(\frac{T_w - T_{in}}{T_w - T_{out}}\right), \tag{8}$$

where v is the free-stream velocity, ρ is the density of the air, L is the major axis of the ellipse chosen as the characteristic length, μ is the dynamic viscosity of air, h is the heat transfer coefficient, k is the thermal conductivity of air, $\dot{m}$ is the mass flow rate, c_p is the heat capacity of air, A_w is the heat transfer area, T_w is the temperature of the tube walls, T_{in} is the temperature at the inlet and T_{out} is the temperature at the outlet.

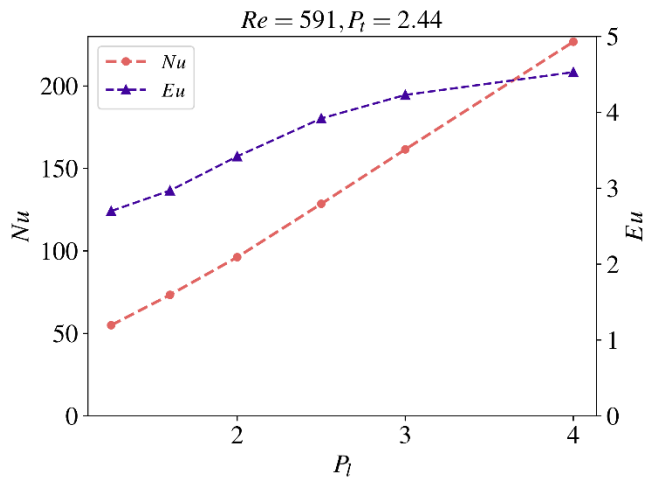

Figure 4: Variation of Nusselt number and Euler number with longitudinal pitch ratio.

Figure 4 represents the variation of Nusselt number and Euler number with longitudinal pitch ratio for the flow conditions of the case study, corresponding to a Reynolds number of 591. It can be observed from Figure 4 that by increasing the longitudinal pitch ratio, both the Nusselt number and the Euler number increase. Therefore, for a given tube shape, it can be observed that minimizing pressure drop and maximizing heat transfer rate exhibit opposite trends, thus, emphasising the need of an optimization algorithm to find an optimum trade-off between the two objective functions.

5.3. Optimization results

The baseline geometry of the tube bundle in Figure 3 is optimized as per the optimization problem represented in Eqns. (2)-(4). The optimization variables were the longitudinal pitch and tube shape parameters (leading and trailing edge radii, major axis length, and tube thickness along the major axis). The geometric constraint was computed using the shoe-lace method as reported in Ref. [14]. The optimization was performed on a workstation with Intel Xeon processor Gold 5220R (2.2 GHz) processor. The computational cost per design step was approximately 90 mins using 24 cores, which consume a maximum of 4 GB of memory.

The optimization history of the problem is illustrated in Figure 5, where the non-dimensional objective and constraint values are plotted for each design step. It can be observed that the objective function is reduced by ~29% while maintaining the heat transfer rate at the 97% of its baseline value. Furthermore, Figure 5 also presents the tube shapes of the design solution exhibiting this performance improvement. The total height of the optimum tubes is 18.4% smaller than in the baseline design while the width of the tube is 18.67% larger. Additionally, the longitudinal pitch ratio is decreased by 25% reducing the total volume of the tube bundle.

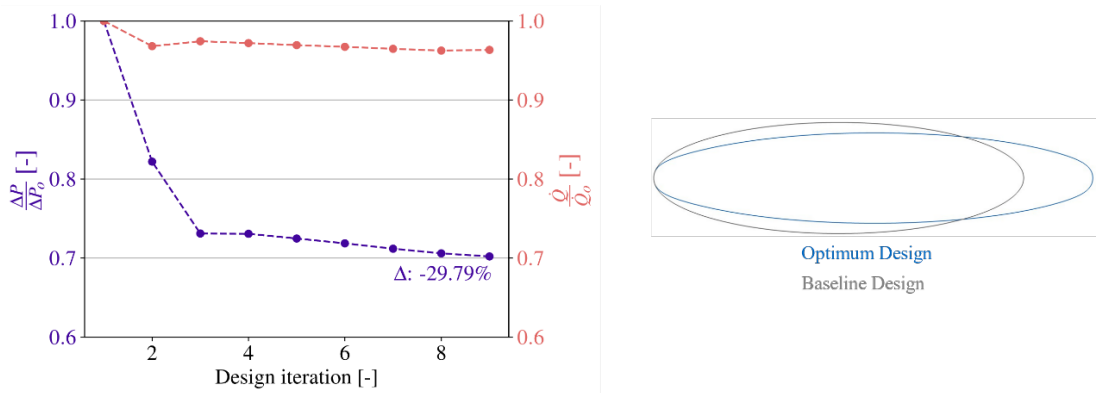

Figure 5: Optimization history depicting the evolution of the normalized objective function and constraint values (Left). Comparison of the optimum tube shape and the baseline design (Right).

The optimum and baseline geometry are compared in Figure 6, which also shows the corresponding velocity contours obtained from the CFD simulations. It can be observed that the maximum velocity is reduced in the optimum geometry as compared to the baseline case. The reduction in the maximum velocity is ~11%. This is due to the reduction in the frontal area of the optimum design, which provides a larger flow passage area. Consequently, this leads to a lower maximum velocity and subsequently to a lower pressure drop. The flow patterns in the optimum design result in smaller recirculation zone between the tubes, see Figure 6. On the other hand, the wake after the last tube is longer compared to that of the baseline. A larger wake region in the optimum geometry can be attributed to a slower flow diffusion due to the lower maximum flow velocity when compared with the baseline.

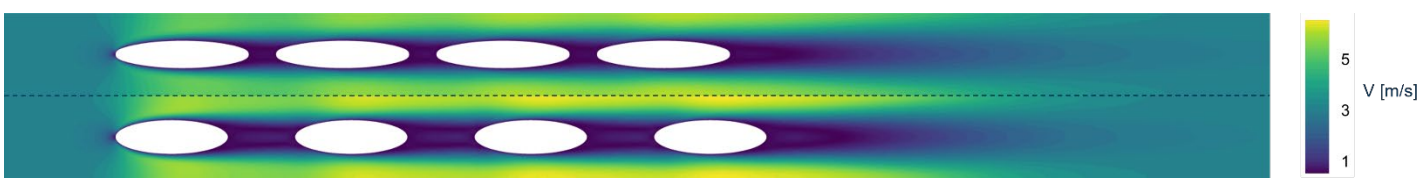

Figure 6: Velocity contours for the optimum design (top) and the baseline design (bottom).

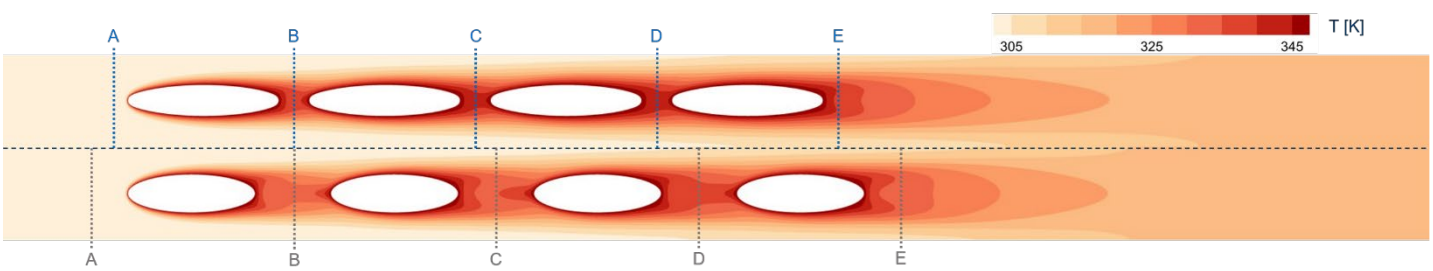

Figure 7: Temperature contours for the optimum design (top) and the baseline design (bottom) with the locations of lines A-E for quantitative comparisons.

The temperature distribution in the air flow for the baseline and the optimum geometry is shown in Figure 7. Since the total heat transfer rate is constrained, the overall increase in fluid temperature between the inlet and the outlet is similar in the two cases. However, the local distribution, especially in the wake of the tubes, is different. For a quantitative comparison, the velocity magnitude, pressure, and temperature in the airflow are sampled at 5 locations (A-E) as shown in Figure 7. These locations are arranged such that locations B, C, and D, are at the centre of space between the consecutive tubes.

Figure 8 compares the air velocity, pressure, and temperature distributions between the two designs at the locations A-E. The largest pressure drop occurs in both cases across the first tube, see the pressure distributions in Figure 8. The optimum design exhibits a lower pressure drop across the tubes compared to the baseline design due to the lower flow blockage, which leads to a more uniform velocity distribution. Conversely, the temperature spread along the vertical direction increases, with the maximum temperature occurring at the center of the recirculating region, which can be 6 K higher than in the baseline case.

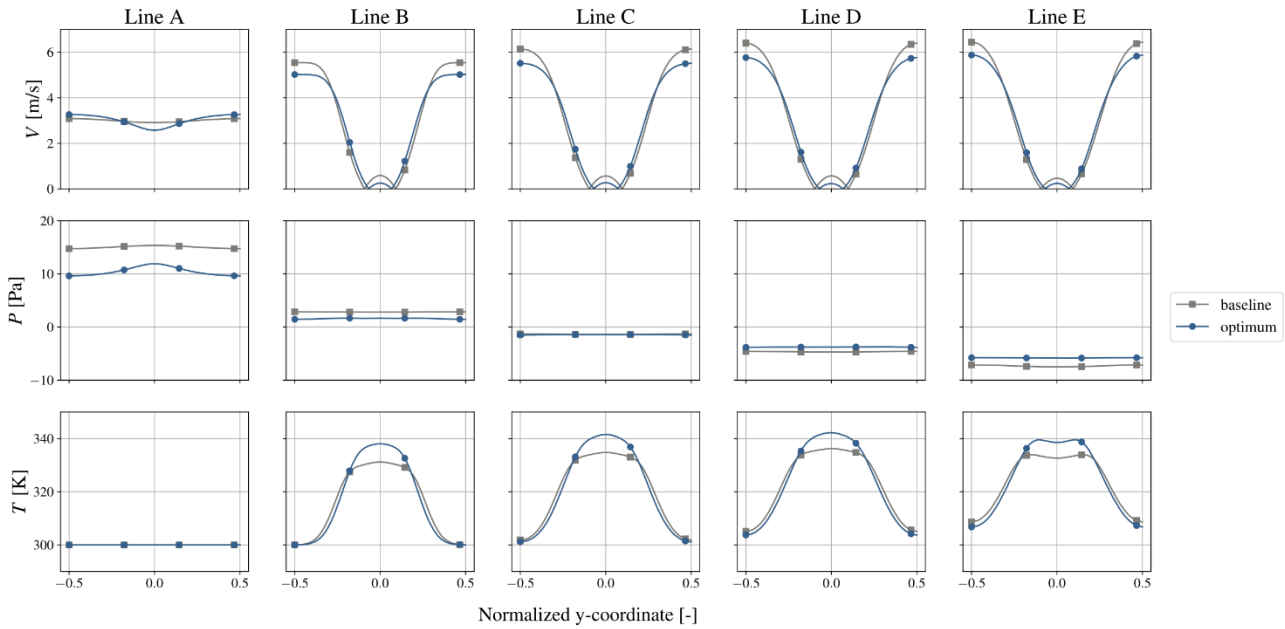

Figure 8: Comparison of the baseline and optimum designs with respect to the variation of flow properties – velocity magnitude, pressure, and temperature – as a function of the normalized y-coordinate at the locations A-E.

The longitudinal pitch ratio (P_l) is reduced from 1.6 to 1.2 by the automated design chain. This reduction in the longitudinal pitch leads to a decrease in pressure drop similar to the trend observed in the parametric study. It should be noted, however, that the large change in pitch during the design optimization deteriorates the quality of the mesh obtained after the geometry adaptation imposed by the optimizer.

Overall, this study demonstrates that the simultaneous optimization of the tube shape and longitudinal pitch using the adjoint-based framework proposed in this study, can substantially improve the performance of in-line bare-tube heat exchangers with relatively low computational cost.

6. Conclusion

In this work, an adjoint-based design optimization method using CAD-based parametrization was developed for optimizing the tube shape and layout of bare-tube heat exchangers. The CFD model was validated against experimental data in the literature and was used for a parametric study to investigate the effect of longitudinal pitch on the performance of in-line tube bundles. Moreover, the developed optimization framework was applied to optimize an exemplary in-line elliptical tube bundle to reduce the pressure drop across the heat exchanger while constraining the heat transfer rate. Results showed that optimizing the tube shape and longitudinal pitch simultaneously results in a performance improvement of more than 29%, while satisfying the imposed constraint on the heat transfer rate.

Future work will include transverse pitch in the optimization framework and extend the problem to more realistic three-dimensional problems.

Acknowledgements

Special thanks to Dr. Matteo Pini and Prof. Piero Colonna for their guidance. Acknowledgment is extended to both VITO and TU Delft for providing the computational resources.

References

[1] B. Sundén and J. Fu, "Chapter 6 - Aerospace Heat Exchangers," in *Heat Transfer in Aerospace Applications*, Academic Press, 2017, pp. 89–115, doi: 10.1016/b978-0-12-809760-1.00006-5.

[2] H. Lim, U. Han, and H. Lee, "Design optimization of bare tube heat exchanger for the application to mobile air conditioning systems," *Appl. Therm. Eng.*, vol. 165, June 2019, 114609, 2020, doi: 10.1016/j.applthermaleng.2019.114609.

[3] Z. Huang, J. Ling, Y. Hwang, V. Aute, and R. Radermacher, "Airside Heat Transfer and Friction Characteristics of a 0.8 mm Diameter Bare Tube Heat Exchanger," *Heat Transf. Eng.*, vol. 41:19–20, pp. 1720–1730, 2020, doi: 10.1080/01457632.2019.1640474.

[4] D. Bacellar, V. Aute, Z. Huang, and R. Radermacher, "Design optimization and validation of high-performance heat exchangers using approximation assisted optimization and additive manufacturing," *Sci. Technol. Built Environ.*, vol. 23, no. 6, pp. 896–911, 2017, doi: 10.1080/23744731.2017.1333877.

[5] J. Tancabel, V. Aute, and R. Radermacher, "Review of Shape and Topology Optimization for Design of Air-to-Refrigerant Heat," *Int. Refrig. Air Cond. Conf.*, Paper 1965, 2018.

[6] G. P. Merker and H. hanke, "Heat transfer and pressure drop on the shell-side of tube-banks having oval-shaped tubes," *Int. J. Heat Mass Transf.*, vol. 29, no. 12, pp. 1903–1909, 1986, doi: 10.1016/0017-9310(86)90008-6.

[7] R. S. Matos, J. V. C. Vargas, T. A. Laursen, and F. E. M. Saboya, "Optimization study and heat transfer comparison of straggered circular and elliptic tubes in forced convection," *Int. J. Heat Mass Transf.*, vol. 44, no. 20, pp. 3953–3961, 2001, doi: 10.1016/S0017-9310(01)00006-0.

[8] R. Deeb, "Correlations and numerical analysis of thermal-hydraulic performance of staggered mixed tube bundle composed of circular and drop-shaped tubes," *Int. J. Heat Mass Transf.*, vol. 199, 2022, doi: 10.1016/j.ijheatmasstransfer.2022.123487.

[9] G. Stanescu, A. J. Flower, and A. Bejan, "The optimal spacing for cylinders in crossflow forced convection," *J. Heat Transfer*, vol. 117, no. 3, pp. 767–770, 1995, doi: 10.1115/1.2822645.

[10] A. Safwat Wilson and M. Khalil Bassiouny, "Modeling of heat transfer for flow across tube banks," *Chem. Eng. Process. Process Intensif.*, vol. 39, no. 1, pp. 1–14, 2000, doi: 10.1016/S0255-2701(99)00069-0.

[11] N. Kasagi, N. Shikazono, Y. Suzuki, and T. Oku, "Assessment of High-Performance Micro Bare-Tube Heat Exchangers for Electronic Equipment Cooling," *Proc. Therm. Eng. Conf.*, 2003, doi: 10.1299/jsmeted.2003.447.

[12] N. Anand, S. Vitale, M. Pini, and P. Colonna, "Assessment of FFD and CAD-based shape parametrization methods for adjoint-based turbomachinery shape optimization," *Proc. Montr. 2018 Glob. Power Propuls. Forum*, p. 135, 2018.

[13] R. Agromayor, N. Anand, J. D. Müller, M. Pini, and L. O. Nord, "A Unified Geometry Parametrization Method for Turbomachinery Blades," *CAD Comput. Aided Des.*, vol. 133, p. 102987, 2021, doi: 10.1016/j.cad.2020.102987.

[14] P. Pai Raikar, N. Anand, M. Pini, and C. De Servi, "Concurrent optimization of multiple heat transfer surfaces using adjoint-based optimization with a CAD-based parametrization," *Int. J. Heat Mass Transf. (In Prep.)*, 2024.

[15] F. Palacios, M. R. Colonno, A. C. Aranake, A. Campos, S. R. Copeland, T. D. Economon, A. K. Lonkar, T. W. Lukaczyk, T. W. R. Taylor and J. J. Alonso, "Stanford University Unstructured (SU2): An open-source integrated computational environment for multi-physics simulation and design," *51st AIAA Aerosp. Sci. Meet. Incl. New Horizons Forum Aerosp. Expo. 2013*, no. January, pp. 1–60, 2013, doi: 10.2514/6.2013-287.

[16] D. Kraft, "A Software Package for Sequential Quadratic Programming," *Technical Report DFVLR-FB*, vol. 88, no. 28. pp. 1–33, 1988.

[17] P. Virtanen, R. Gommers, T. E. Oliphant and SciPy 1.0 Contributors, "SciPy 1.0: Fundamental Algorithms for Scientific Computing in Python," *Nat. Methods*, vol. 17, pp. 261–272, 2020, doi: 10.1038/s41592-019-0686-2.